

Responsive Microgrooves for the Formation of Harvestable Tissue Constructs

Halil Tekin,^{†,‡,§,¶} Gozde Ozaydin-Ince,^{||,¶} Tonia Tsinman,[‡] Karen K. Gleason,^{||} Robert Langer,^{*,§,||,⊥} Ali Khademhosseini,^{*,‡,⊥,¶} and Melik C. Demirel^{*,||,¶,▽}

[†]Department of Electrical Engineering and Computer Science, Massachusetts Institute of Technology, 77 Massachusetts Avenue, Cambridge, Massachusetts 02139, United States

[‡]Department of Medicine, Center for Biomedical Engineering, Brigham and Women's Hospital, Harvard Medical School, Boston, Massachusetts 02115, United States

[§]David H. Koch Institute for Integrative Cancer Research, Massachusetts Institute of Technology, Building 76-661, 77 Massachusetts Avenue, Cambridge, Massachusetts 02139, United States

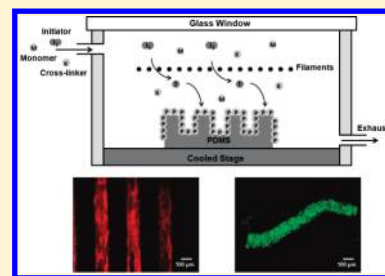
^{||}Department of Chemical Engineering, Massachusetts Institute of Technology, Cambridge, Massachusetts 02139, United States

[⊥]Harvard–MIT Division of Health Sciences and Technology, Massachusetts Institute of Technology, Cambridge, Massachusetts 02139, United States

[¶]Wyss Institute for Biologically Inspired Engineering, Harvard Medical School, Boston, Massachusetts 02138, United States

[▽]Materials Research Institute and Department of Engineering Science, Pennsylvania State University, University Park, Pennsylvania 16802, United States

ABSTRACT: Given its biocompatibility, elasticity, and gas permeability, poly(dimethylsiloxane) (PDMS) is widely used to fabricate microgrooves and microfluidic devices for three-dimensional (3D) cell culture studies. However, conformal coating of complex PDMS devices prepared by standard microfabrication techniques with desired chemical functionality is challenging. This study describes the conformal coating of PDMS microgrooves with poly(*N*-isopropylacrylamide) (PNIPAAm) by using initiated chemical vapor deposition (iCVD). These microgrooves guided the formation of tissue constructs from NIH-3T3 fibroblasts that could be retrieved by the temperature-dependent swelling property and hydrophilicity change of the PNIPAAm. The thickness of swollen PNIPAAm films at 24 °C was approximately 3 times greater than at 37 °C. Furthermore, PNIPAAm-coated microgroove surfaces exhibit increased hydrophilicity at 24 °C (contact angle $\theta = 30^\circ \pm 2$) compared to 37 °C ($\theta = 50^\circ \pm 1$). Thus PNIPAAm film on the microgrooves exhibits responsive swelling with higher hydrophilicity at room temperature, which could be used to retrieve tissue constructs. The resulting tissue constructs were the same size as the grooves and could be used as modules in tissue fabrication. Given its ability to form and retrieve cell aggregates and its integration with standard microfabrication, PNIPAAm-coated PDMS templates may become useful for 3D cell culture applications in tissue engineering and drug discovery.



INTRODUCTION

Poly(dimethylsiloxane) (PDMS) is widely used for fabrication of complex three-dimensional (3D) or high aspect ratio microstructures and devices due to its physicochemical properties. Elasticity, ease of processing, biocompatibility, and mechanical stability of PDMS¹ makes it a desirable substrate to fabricate microdevices for biomedical applications such as cell culture,^{2,3} drug toxicity, and metabolism screening.⁴ Recently, PDMS has also been used as a stretchable “organ-on-a-chip” device,⁵ which could potentially replace expensive animal testing.

PDMS possesses high gas and liquid permeability coefficients due to its large free volume, and low selectivity.¹ Although this may be advantageous for a range of applications, the ability to control the permeability of PDMS surfaces is desirable to prevent the leakage of hydrophobic drugs or metabolites in drug toxicity

and metabolism screening. In addition, the ability to reversibly change PDMS substrate properties may be of interest for a range of cell culture applications. Therefore, simple approaches of modifying PDMS substrates while maintaining its mechanical and optical properties are desirable.⁶ Strategies for coating pores or microchannels involve vapor phase deposition of crystalline (e.g., parylene^{7,8}) or amorphous polymers (e.g., poly(2-hydroxyethyl methacrylate) (pHEMA)⁹). A crystalline polymer provides a perfect high barrier for molecular penetration, but it has limited mechanical properties (e.g., stretchability) due to its high modulus (i.e., elastic modulus of 1–10 GPa). An amorphous

Received: January 14, 2011

Revised: March 7, 2011

polymer, on the other hand, is typically used on stretchable devices to complement the low modulus (i.e., 1–100 MPa) of PDMS, but the molecular pores of the amorphous phase should be engineered to gain high barrier properties for moisture as well as chemicals. The latter could be achieved easily, in vapor phase coatings, by adjusting the cross-linker density of the polymer.¹⁰

A few studies have been conducted to fabricate tissue constructs (e.g., cell detachment,¹¹ mechanical conditioning, and cell detachment¹²) using poly(*N*-isopropylacrylamide) (PNIPAAm)-grafted PDMS.¹² PNIPAAm is a stimuli-response polymer that undergoes a dramatic change in surface energy at its lower critical solution temperature (LCST) of approximately 32 °C. At temperatures above the LCST, PNIPAAm dehydrates and changes its conformation to a collapsed form,¹³ which is suitable for cell adhesion and culture at 37 °C. Below the LCST, it swells and hydrates in aqueous solution,¹³ which drives cell detachment with conditioned extracellular matrix (ECM) from the culture surface without disturbing cell–cell and cell–ECM interactions.^{14–17} Surface-grafted PNIPAAm was also used for temperature controlled release of biofilms from the substrates.¹⁸ Thermoresponsive substrates with microgroove patterns were fabricated to form harvestable cell sheets¹⁹ or capillary networks.²⁰ Microgroove patterns can be potentially useful to align the cells along the channel direction and initiate cytoskeletal organization to form physiologically active modular tissue constructs. In these studies, PNIPAAm was grafted in liquid phase on microgrooves to tune surface energy. However, conformal grafting of PNIPAAm in liquid phase was difficult to achieve. Recently, PNIPAAm-based hydrogel microstructures were fabricated using a soft lithographic approach; however, these microstructures exhibit temperature-dependent shape changes that apply mechanical forces on the resulting tissue constructs and may deform the final aggregate shapes.²¹

Microtextured surfaces were previously coated with PNIPAAm using electron-beam polymerization in liquid phase.²⁰ This method has led PNIPAAm to agglomerate nonuniformly in groove patterns and caused rounded shape ridges. The overall process has produced a nonuniform PNIPAAm coating on the substrates, which can adversely affect the cell orientation and tissue formation within grooves. Herein, we created a conformal PNIPAAm coating on PDMS using the initiated chemical vapor deposition (iCVD) technique. iCVD is a free radical polymerization technique to produce structurally well-defined conformal polymer coatings, and therefore offers a high degree of control over the geometry and thickness of the polymer.¹⁰ While traditional approaches require substrates that possess specific functional groups and produce films of limited thickness, the iCVD method can be applied to virtually any substrate and can result in film thicknesses ranging from a few nanometers to a few micrometers.^{10,22} The iCVD process occurs in a single step, and growth rates can exceed 100 nm/min.²² We used a growth rate of ~6 nm/min to create ~300 nm conformal PNIPAAm coating on PDMS substrates.

We showed that the conformal coating of PDMS microgrooves with PNIPAAm created using iCVD can be used to form geometrically controlled longitudinal tissue constructs and enable their further retrieval in a temperature-dependent manner by exploiting the swelling/deswelling property and tunable hydrophilicity of the responsive polymer. This stimuli-responsive template can be useful in fabricating modular tissue units for tissue engineering applications and potentially integrated within microfluidic devices.

MATERIALS AND METHODS

Materials. Silicon elastomer and curing agent were purchased from Dow Corning Corporation (Midland, MI). Dulbecco's phosphate buffered saline (PBS), calcein-AM and ethidium homodimer, Dulbecco's modified Eagle's medium (DMEM), fetal bovine serum (FBS), penicillin-streptomycin (Pen-strep), and Alexa-Fluor 594 phalloidin were all purchased from Invitrogen (Carlsbad, CA). Glass slides and ethanol were purchased from Fisher Scientific (Fair Lawn, NJ). The monomer, *N*-isopropylacrylamide (NIPAAm) (97%), the initiator, *tert*-butyl peroxide (TBPO) (98%, Aldrich), trichlorovinylsilane, fluorescein isothiocyanate-conjugated bovine serum albumin (FITC-BSA), bovine serum albumin (BSA), and TritonX-100 were all purchased from Sigma-Aldrich Chemical Co. (St. Louis, MO). Paraformaldehyde was purchased from Electron Microscopy Sciences (Hatfield, PA). The cross-linker, ethylene glycol diacrylate (EGDA) (98%) was purchased from Polysciences Company (Warrington, PA). Silicon (Si) wafers were purchased from University Wafer (Boston, MA).

Fabrication of PDMS Microgrooves. Silicon masters with longitudinal patterns were developed with SU-8 photolithography and used as templates to fabricate PDMS replicas. PDMS microgrooves were formed by curing a mixture of 10:1 silicon elastomer and curing agent at 70 °C for 2 h and then detached from silicon masters. The channel depth and width of the resulting PDMS microgrooves were adjusted to ~150 μ m. The space between two channels was ~150 μ m.

PNIPAAm Coating with iCVD. PDMS substrates were treated before iCVD to provide covalent bonding of PNIPAAm to the surface. The PDMS surfaces were first treated with oxygen plasma for 30 s. After the plasma treatment, the PDMS surfaces were immediately placed in an oven at 40 °C together with 5 mL of trichlorovinylsilane. The samples were kept in the oven for 4 min, giving them sufficient time to react with the silane. Following this treatment, the samples were directly placed in the iCVD reactor for deposition. The iCVD of PNIPAAm were performed in a custom-built deposition reactor with a base pressure of 1 mTorr as illustrated in Figure 1a. The monomer and the cross-linker were heated in separate glass jars to 75 and 80 °C respectively and delivered into the reactor using needle valves. The initiator was kept at room temperature, and delivery into the reactor was achieved by using a mass flow controller. Nitrogen gas was used as a patch flow. A filament array of 14 parallel chrome alloy filaments was used for thermal decomposition of the initiator molecules. A back-side cooled sample stage kept the temperature of the sample constant. The thickness of the deposited films was monitored in real-time using a He–Ne laser interferometry setup, in which the laser beam entered the reactor from the top quartz window and reflected from the sample surface. The thickness measurements were performed on Si-wafers that were located next to PDMS samples in the reactor. The thickness of the film was calculated from the beam intensity oscillations. The iCVD deposition of 300 nm thick PNIPAAm was performed at 100 mTorr pressure, and the sample and filament temperatures were kept constant at 30 and 250 °C, respectively. The flow rates of NIPAAm, EGDA, TBPO, and N₂ were maintained at 5, 1, 1, and 1 sccm, respectively. At these conditions the growth rate was ~6 nm/min. PNIPAAm reacts with the vinyl bonds of the silane on PDMS surface. Without silane treatment, PNIPAAm can form a conformal thin film without covalent bonding, which has weaker adhesion compared to the silanized surface.

Characterization. Surface modification of the PNIPAAm-deposited PDMS surface was analyzed by Fourier transform infrared spectroscopy with attenuated total reflection (FTIR-ATR). The spectra were recorded by using a Bruker Alpha FTIR. An uncoated PDMS surface was used as the control. Chemical characterization of the deposited films on a Si-wafer was done using a Nexus 870 FTIR (Thermo Nicolet) equipped with a DTGS-TEC detector. The spectra were acquired at 4 cm⁻¹ resolution, and the number of scans was kept at 128. The spectrum of a bare Si wafer was used as the background.

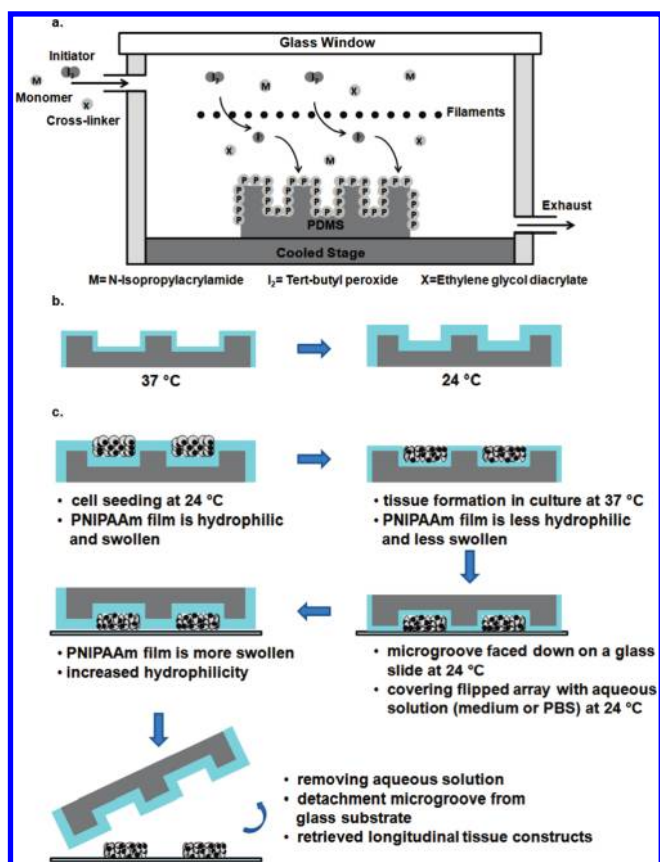


Figure 1. Schematic of (a) PNIPAAm coating on PDMS microgrooves by iCVD; (b) swelling of PNIPAAm film on PDMS microgrooves at physiological (37 °C) and ambient temperature (24 °C); and (c) formation and retrieval process of longitudinal tissue constructs.

Scanning Electron Microscopy. PNIPAAm coated microgrooves were dried at room temperature. The samples were subsequently mounted onto aluminum stages, sputter coated with gold, and analyzed under scanning electron microscopy (SEM) (JEOL JSM 6060) at a working distance of 4 mm.

Atomic Force Microscopy. Surface topography of uncoated and PNIPAAm-coated PDMS samples was determined by using an atomic force microscope (AFM) (Nanoscope V, Veeco Inc.). AFM images were obtained in tapping mode using rectangular shaped silicon nitride cantilevers. The root-mean-square (rms) value of the surface roughness for flattened images was quantified by using the software equipped with Nanoscope V.

Contact Angle Measurement and Swelling Test. Static contact angle measurements was performed with deionized water (10 μ L droplet) using a contact angle measuring instrument (FTA 1000B, First Ten Angstroms, Inc., Portsmouth, VA). To analyze the swelling properties, Si wafers were coated with \sim 300 nm PNIPAAm, and water swelling of the PNIPAAm films was then monitored in real-time using an interferometry setup (J.A. Woollam, Inc. Lincoln, NE).

Cell Culture. NIH-3T3 fibroblasts were cultured in medium containing 89% DMEM, 10% FBS, and 1% penicillin-streptomycin and passaged every 3 days. Cells were maintained at 37 °C in a 5% CO₂ humidified incubator.

Cell Adhesion and Protein Adsorption on PNIPAAm-Coated PDMS Surfaces. PNIPAAm-coated PDMS surfaces, a bare PDMS surface, and a bare glass slide were rinsed with ethanol, and kept in PBS until cell seeding. NIH-3T3 fibroblasts were trypsinized and prepared in culture medium. All samples were immersed in 6 mL of a cell

solution containing 2.5×10^5 cells/mL. Cell adhesion on PNIPAAm-coated surfaces was performed at 37 °C for 2 h and 24 °C for 2 h, while the bare PDMS surface and glass slide were only subjected to 37 °C for 2 h. After incubation at experimental temperatures, all samples were dipped into PBS to remove nonadherent cells. Samples were visualized with an inverted microscope (Nikon Eclipse TE2000-U), and adherent cells were counted.

FITC-BSA was dissolved in PBS at a density of 25 μ g/mL. To test the protein adsorption to PNIPAAm-coated PDMS surfaces, the bare PDMS surface, and the bare glass slide, 200 μ L of the protein solution was evenly distributed on the surfaces. PNIPAAm-coated surfaces were incubated at 37 °C for 2 h and 24 °C for 2 h, while the bare PDMS surface and glass slide were only subjected to 37 °C for 2 h. After incubation, samples were washed with PBS and analyzed under an inverted fluorescent microscope (Nikon Eclipse TE2000-U). Fluorescent images were analyzed using ImageJ software.

Cell Seeding on Microgrooves and Formation of Longitudinal Tissues. PNIPAAm-coated microgrooves were placed in six-well culture plates after fabrication, rinsed with ethanol, and kept in PBS until cell seeding. NIH-3T3 fibroblasts were trypsinized and prepared in culture medium. Microgrooves were kept at room temperature for at least 30 min to make the surface hydrophilic for better cell-seeding conditions at 24 °C. After aspirating PBS from each six-well plate, a suspension of NIH-3T3 fibroblasts was seeded on each microgroove array at a density of $\sim 2.7 \times 10^5$ cells/cm² and kept at ambient temperature for 20 min to drive spreading of the cell suspension on the surface. Subsequently, microgroove arrays were gently washed with PBS to remove undocked cells on the microgroove surface and immersed in fresh culture medium. Seeded microgroove arrays were kept in a 5% CO₂ humidified incubator at 37 °C for 3 days. Microscope images were taken daily to analyze longitudinal tissue formation in the microgrooves.

To analyze cytoskeletal organization in microgrooves after 3 days of incubation, F-actin fibrils in the cells within formed tissue constructs were stained with phalloidin. Samples were first fixed with 4% paraformaldehyde for 10 min at room temperature and then rinsed two times with PBS. Cells were permeabilized with 0.1% TritonX-100 for 5 min at room temperature and washed two times with PBS. Samples were then incubated in a PBS solution containing 1% BSA and Alexa-Fluor 594 Phalloidin (1:40 dilution in PBS after dissolving stock powder in 1.5 mL methanol) for 1 h at room temperature. Samples were finally washed three times with PBS and visualized under an inverted fluorescent microscope (Nikon Eclipse TE2000-U).

Live/Dead Staining. Live/dead solution was prepared with 2 mM of calcein-AM and 4 mM of ethidium homodimer in PBS. For live and dead evaluation, each microgroove was placed in live/dead solution during deposition on a glass substrate for a maximum of 30 min at 24 or 37 °C. Live cells were stained by calcein-AM with fluorescent green color, while homodimer stained dead cells with fluorescent red color. Cells were analyzed under an inverted microscope (Nikon Eclipse TE2000-U).

Retrieval of Modular Longitudinal Tissue Constructs. After culturing cell-seeded microgroove arrays for 3 days, longitudinal tissue constructs were retrieved from the microgrooves by deposition of the arrays on glass slides, as shown in Figure 1c. For release experiments at 24 °C, microgroove arrays ($n = 3$) were gently placed on a glass slide and immersed in 24 °C PBS for 30 min with the grooves facing down. Control experiments for microgroove arrays ($n = 3$) with the same method were performed at 37 °C for 30 min to test whether the temperature was the main driving force in releasing the tissue constructs from the microgrooves. For control experiments at 37 °C, microgrooves were covered with 37 °C PBS. Phase images for each sample were taken using an inverted microscope (Nikon Eclipse TE2000-U). Approximate lengths of retrieved tissue constructs were measured with Spot

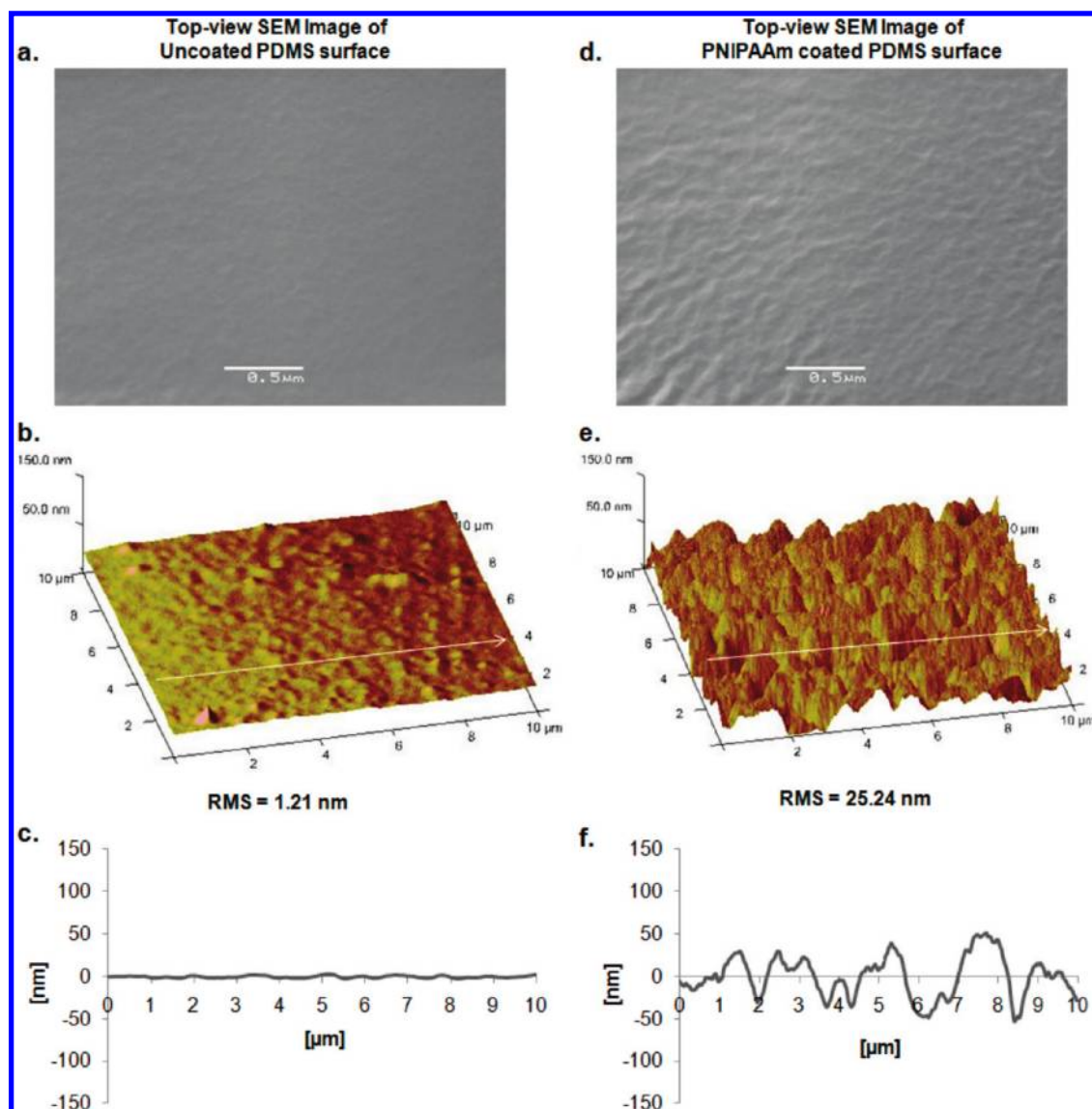


Figure 2. (a) SEM image and (b) AFM image showing surface topography of uncoated PDMS surface. Surface analysis for flattened AFM image of bare PDMS surface gives an rms value of 1.21 nm. (c) Height change for uncoated PDMS surface through the arrow direction. (d) SEM image and (e) AFM image showing surface topography of a PNIPAAm-coated PDMS surface. Surface analysis for the PNIPAAm-coated PDMS surface exhibits an rms value of 25.24 nm. (f) Height change over the topography of the PNIPAAm-coated PDMS surface through the arrow direction.

Advanced software to determine the frequency of tissue lengths for released modular tissue constructs from PNIPAAm-coated micro-grooves at 24 °C.

Statistical Analysis. Data was shown as the mean and \pm standard deviation (\pm sd). Statistical analysis was performed with an unpaired Student's *t* test, and $p < 0.05$ was considered significant.

RESULTS AND DISCUSSION

PNIPAAm Coating on PDMS Substrates. PNIPAAm coating on PDMS substrates with the iCVD method was performed in a custom built deposition reactor as illustrated in Figure 1a. The as-deposited thickness of the responsive film was adjusted to be ~ 300 nm. The coating thickness on the samples varied ± 10 nm, while thickness variation among 4 samples was ± 20 nm. The swelling of the responsive film was observed as illustrated in Figure 1b. To observe the effect of PNIPAAm coating on surface

roughness, SEM and tapping-mode AFM images were taken for the bare PDMS surface (Figure 2a,b) and the PNIPAAm-coated PDMS surface (Figure 2d,e). Top-view SEM images, AFM images, and plots of corresponding height change (Figure 2c,f) showing surface topographies demonstrated that PNIPAAm coating on the surface caused increased roughness. The rms values reveal the degree of surface roughness. The rms value of the PNIPAAm-coated PDMS surface (25.24 nm) is significantly higher than that of the bare PDMS surface (1.21 nm), suggesting that PNIPAAm coating on PDMS surfaces were more rough compared to bare PDMS substrates.

We also analyzed the chemical properties of PNIPAAm deposition using FTIR characterization. Figure 3a shows the FTIR spectra of the PNIPAAm-coated PDMS surfaces as well as noncoated PDMS substrates. FTIR peaks for the PNIPAAm coated surfaces show O–H stretching at $3700\text{--}3050\text{ cm}^{-1}$ for NIPAAm as well as C=O stretching at $1750\text{--}1690\text{ cm}^{-1}$ for

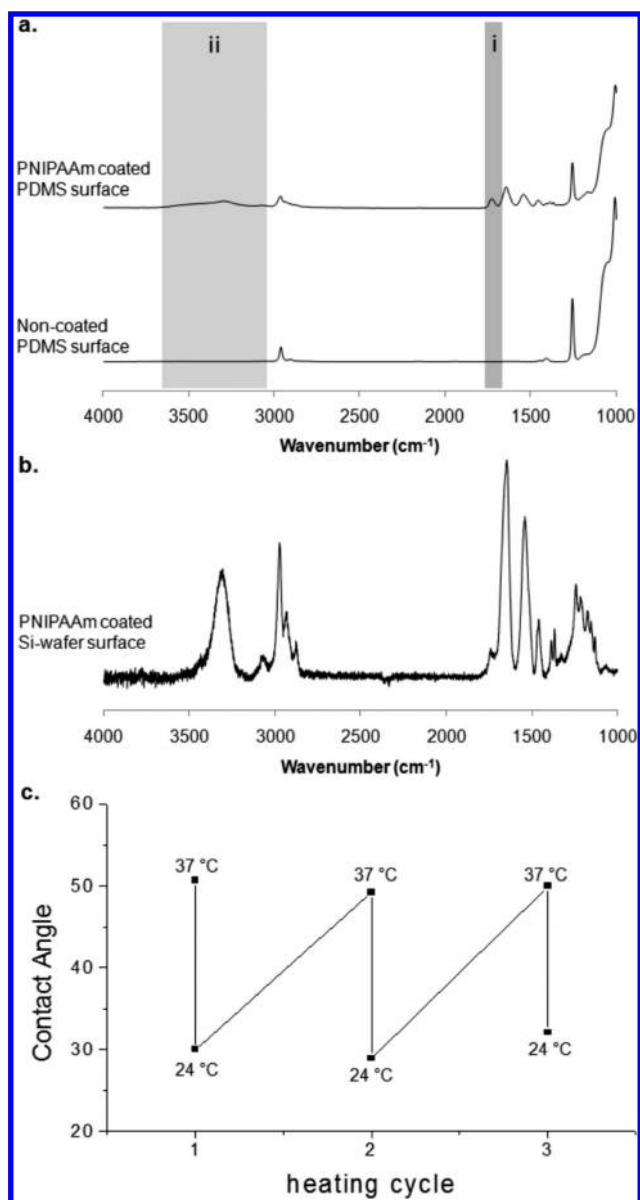


Figure 3. (a) The FTIR spectra for iCVD PNIPAAm on PDMS (top) and bare PDMS (bottom). The shaded regions correspond to (i) C=O stretching at 1750–1690 cm⁻¹ for EGDA and (ii) O–H stretching at 3700–3050 cm⁻¹ for NIPAAm. Additionally, the amide I (~1660 cm⁻¹) and amide II (~1530 cm⁻¹) bands are visible in both iCVD-coated PDMS and in (b) FTIR spectra for iCVD PNIPAAm on a Si-wafer substrate. The absence of peaks due to unsaturated carbon at 1640–1660 cm⁻¹ for PNIPAM shows the complete reaction of the vinyl bonds. (c) Contact angle results for PNIPAAm film for three cycles of quick temperature changes between 24 and 37 °C.

EGDA. Figure 3b shows the FTIR spectra of a PNIPAAm-deposited Si-wafer. We note that the absence of peaks in Figure 3b due to unsaturated carbon at 1640–1660 cm⁻¹ for PNIPAM indicates the complete reaction of the vinyl bonds, thus complete polymerization.

To test the changes in surface energy under temperature transformation from 24 and 37 °C, static contact angle measurements were performed for PNIPAAm-coated substrates. Interestingly, the contact angle at 24 °C was measured to be 30° ± 2, while it was 50° ± 1 at 37 °C. Also, the contact angle for the bare

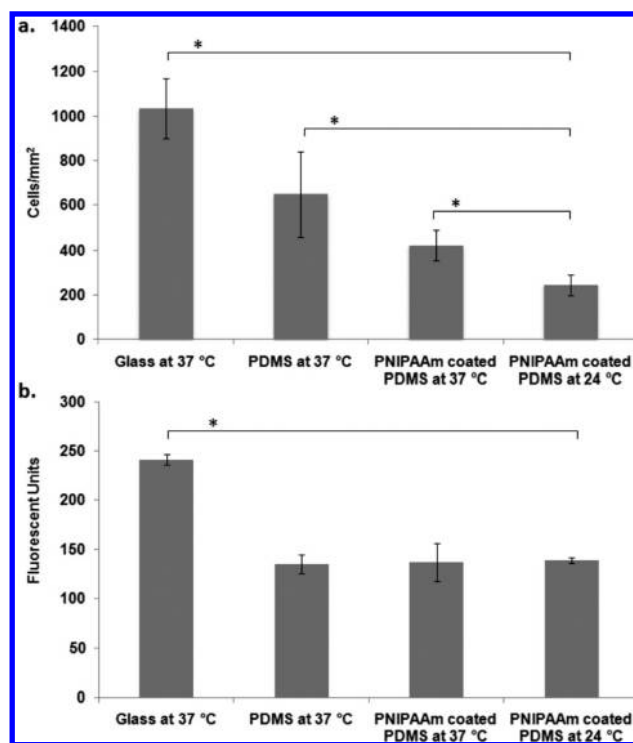


Figure 4. (a) Cell adhesion and (b) protein adsorption on 300 nm of PNIPAAm-coated 2D PDMS surfaces for 2 h incubation at 37 °C and at 24 °C and comparison with adhesion on bare PDMS and glass surfaces. * shows a statistically significant difference in variance ($p < 0.05$).

PDMS surface at 24 °C was measured to be 96° ± 4. It was previously shown that contact angle values for bare PDMS do not change significantly between ambient and physiological temperatures.²³ We also tested the repeatability of the temperature-dependent wettability of PNIPAAm films at 24 and 37 °C. The results showed a substantial reversibility for three cycles of quick temperature transformations between 24 and 37 °C (Figure 3c). Furthermore, we observed that volumetric swelling of PNIPAAm film at 24 °C was approximately 3 times greater than at 37 °C. This observation correlates with recent experiments in which it was shown that a PNIPAAm-coated Si-wafer with iCVD exhibited 3 times thickness change in swollen state compared to the dry state below the LCST.²² Conformal PNIPAAm coating on silicon-based substrates demonstrated a significant swelling change and an increased hydrophilicity at room temperature.

Cell Adhesion and Protein Adsorption. To test the cell adhesion on various surfaces, PNIPAAm-coated PDMS surfaces, a bare PDMS surface, and a bare glass slide were immersed in a solution of NIH-3T3 fibroblasts containing 2.5×10^5 cells/mL. Cells adhesion on the PNIPAAm coated PDMS surface at 24 °C was significantly less than that of the control experiments with the same surface and the bare PDMS at 37 °C (Figure 4a). Contact angle results indicate that PNIPAAm-coated PDMS surfaces had a higher degree of hydrophilicity at 24 °C, which may contribute to a lower level of cell adhesion. It was also previously shown that hydrophilic PNIPAAm surfaces drove the cell detachment from the substrate.^{14–17} Another contributing factor to a lower degree of cell adhesion may be due to the increased swelling of the PNIPAAm film on the surface at 24 °C compared to 37 °C. Interestingly, no significant difference was

observed between the number of adhered cells to PNIPAAm coated or noncoated PDMS substrates at 37 °C. Both surfaces were hydrophobic at this temperature. Hydrophobic substrates are attractive for protein adsorption and subsequent cell adhesion.^{24–29} We hypothesize that the adsorption of proteins such as fibronectin from FBS on hydrophobic surfaces may have caused the same tendency of cell adhesion on these substrates. In addition, cells adhered to the glass surface at 37 °C at significantly higher values than all other surfaces.

The protein adsorption on PNIPAAm-coated PDMS surfaces, the bare PDMS surface, and bare glass slide was analyzed by quantifying the fluorescent expression of these surfaces after exposure to fluorescently labeled protein. As shown in Figure 4b, no significant difference was observed between the degrees of FITC-BSA adsorption on a PNIPAAm-coated PDMS surface at 24 °C and at 37 °C, although swelling of PNIPAAm film on the PDMS surface at 24 °C was more than 37 °C. This suggests that proteins adsorbed on PNIPAAm coatings at both temperatures. Interestingly, protein adsorption at 37 °C on bare PDMS surface was similar to that of the PNIPAAm-coated PDMS surface. It was previously reported that proteins may physically adsorb on PDMS with hydrophobic interactions between the protein and PDMS surface.²³ In this study, PNIPAAm film was somewhat swollen at 37 °C. We hypothesize that, for adhesion on PDMS at 37 °C, proteins may have physically adsorbed on PDMS with hydrophobic interactions and, in the case of PNIPAAm coated PDMS, proteins may have diffused into PNIPAAm-coated PDMS through the somewhat hydrated PNIPAAm chains at 37 °C and adsorbed on PDMS substrate with hydrophobic interactions. We also hypothesize that proteins may have diffused into swollen PNIPAAm film at 24 °C and physically adsorbed onto PDMS layer through hydrophobic interactions. In addition, the fluorescent expression of a glass slide at 37 °C was significantly higher than all other substrates.

Cell Seeding and Formation of Longitudinal Tissue Constructs within PNIPAAm-Deposited Microgrooves. Microfabricated platforms were previously shown to be useful for 3D cell culture with controlled alignment and longitudinal tissue formation.^{30–35} This study shows PDMS microgroove patterns functionalized with the deposition of a thermoresponsive polymer and their use in harvestable modular tissue formation. Thermoresponsive films on the microgroove arrays exhibited swelling/deswelling property and had a tunable hydrophilicity that could be useful in controlling the microgroove surface adhesiveness for tissue formation and retrieval. The cell seeding process plays an important role to immobilize cells inside the grooves and prevent cell growth on the ridges. After fabrication, microgroove arrays were kept at room temperature for 30 min to form a swollen polymer film with increased hydrophilicity before cell seeding at 24 °C to prevent cell adhesion on microgroove surfaces. NIH-3T3 fibroblasts were used as the model cell type to form longitudinal tissues in the channels. To generate tissue constructs in the microgrooves, a suspension of NIH-3T3 fibroblasts were pipetted onto microgroove arrays at a density of $\sim 2.7 \times 10^5$ cells/cm² at 24 °C. After 20 min incubation at room temperature to drive spreading of cell suspension on microgroove surfaces, arrays were gently rinsed to remove the nonadhered cells that were not inside the microgrooves. As shown in the day-0 image of Figure 5a, there was no cells adhered on the ridges after the cell-seeding process. Cell-seeded microgroove arrays were placed in the incubator for 3 days to form longitudinal tissues. Figure 5a shows the cell-seeding efficiency

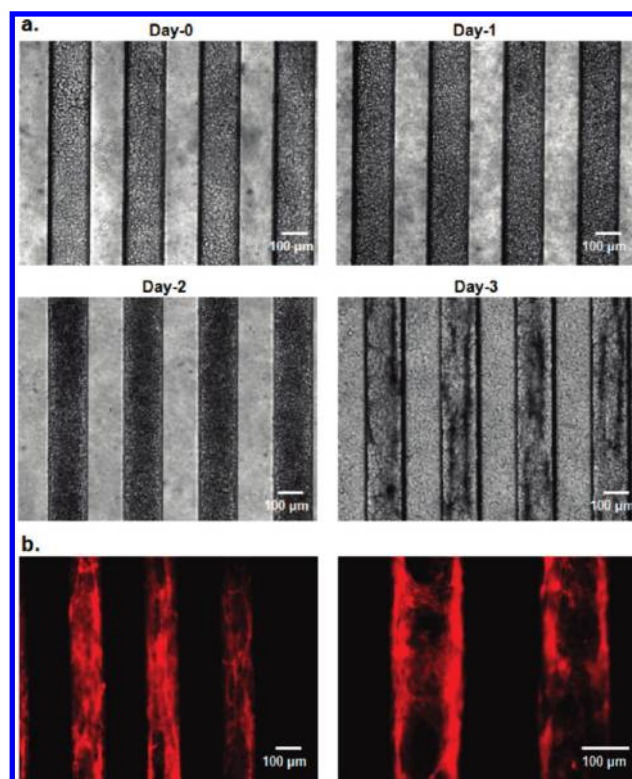


Figure 5. (a) Seeding NIH-3T3 cells onto PNIPAAm-coated microgrooves and formation of longitudinal tissue constructs. (b) Phalloidin staining to visualize F-actin in tissue constructs formed within PNIPAAm-coated microgrooves by day 3.

and tissue formation in PNIPAAm-deposited microgrooves during the 3 day culture. After 1 day in culture, tightly packed cell clusters were observed in many microgrooves, and by 3 days in culture longitudinal tissue fibers were visible in the majority of the grooves. Similar to two-dimensional (2D) cell and protein adhesion experiments, the nonswollen state of the responsive polymer film increases cell adhesion. This contact between cells and the responsive film may increase the stability of the tissue constructs in the microgrooves.

Cell alignment within 3D culture platforms is a crucial element of recreating the tissue complexity of a number of tissues such as muscle.^{33,35} Alignment of the cells was previously achieved with either microfabricated templates^{30–34} or patterning methods.^{35–39} Herein, we analyzed orientation of the cells within the microgrooves after staining their F-actin fibers with phalloidin. Figure 5b illustrates cytoskeletal organization of the cells within longitudinal tissues after 3 days in culture. In the majority of the microgrooves, F-actin filaments in the cells were aligned along the direction of the grooves. Actin fiber intensity and organization show well oriented and interconnected cells within microtissues, suggesting that PNIPAAm deposited templates can be potentially useful to form tissue constructs with controlled alignment and cytoskeletal organization.

Retrieval of Tissue Constructs from PNIPAAm-Deposited Microgrooves. Retrieval of longitudinal tissues is a desirable property of microfabricated culture templates. This study describes a temperature responsive strategy for tissue retrieval from PNIPAAm-deposited PDMS microgrooves by exploiting swelling/deswelling property and hydrophilicity change of responsive polymer film on the substrate. As shown in Figure 1c, for the

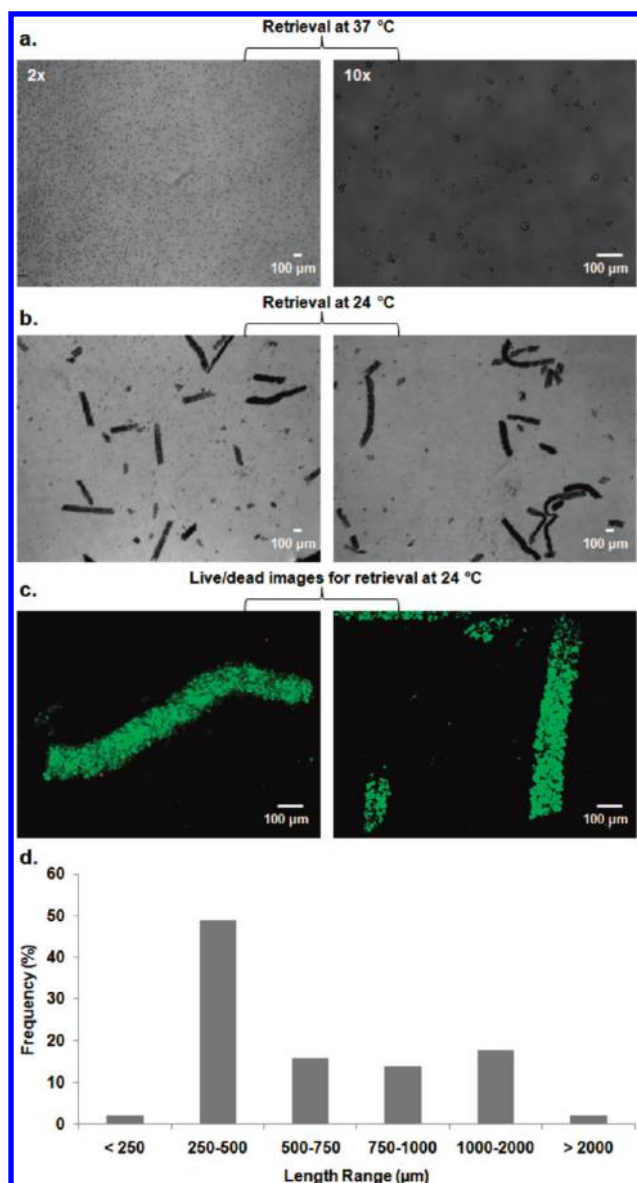


Figure 6. Retrieval of longitudinal tissue constructs from PNIPAAm-coated microgrooves on a glass slide. (a) Phase and live/dead images for control experiment at 37 °C show that only single cells were detached from PNIPAAm coated microgrooves. (b) Low magnification (2 \times) phase contrast images of retrieved tissues from PNIPAAm microgrooves after incubation at 24 °C. (c) Fluorescent images of tissue constructs with live/dead staining. (d) Frequency of lengths of longitudinal tissues retrieved from PNIPAAm-coated microgrooves at 24 °C.

retrieval of microtissues, glass slides were gently placed on the microgroove arrays, and the entire structures were flipped to initiate the detachment of tissue constructs through gravity. Inverted microgrooves were covered with PBS to keep PNIPAAm film in an aqueous environment. Retrieval experiments were performed at 24 and 37 °C. Microgroove arrays were incubated for 30 min at a particular temperature while they were placed face down on a glass slide. After a 30 min incubation, excess solution was removed from the periphery, and the microgroove arrays were gently detached from the glass surface as shown in Figure 1c.

When the retrieval experiment was performed at 37 °C, with PNIPAAm film on the surface in a hydrophilic and less swollen

state, no tissue retrieval was observed from PNIPAAm deposited microgrooves (Figure 6a). In these experiments, only a few individual cells were detached from the arrays as shown in Figure 6a. However, when the procedure was conducted at 24 °C while the PNIPAAm film was in a more hydrophilic and swollen state, microgrooves demonstrated a dramatic increase in retrieval of longitudinal tissues (Figure 6b). Furthermore, we observed high cell viability level based on live/dead staining images for retrieval experiments that were conducted at 24 °C (Figure 6c), suggesting that neither PNIPAAm film deposited on the substrate nor retrieval process adversely affected the cell viability.

Comparison between the results of control experiments at 37 °C and the results of retrieval experiments at 24 °C and considering microgrooves were flipped through gravity at both temperatures suggest that the swelling and hydrophilicity change of the PNIPAAm film on the substrate at two different temperatures is the main cause for the retrieval of the modular tissues. We hypothesize that the higher hydrophilicity of the PNIPAAm film at 24 °C makes the surface undesirable for cell adhesion and initiates cell detachment, and swelling of the PNIPAAm film at 24 °C compared to 37 °C changes the topography of the surface, which can drive subsequent release of tissue constructs from the grooves. During retrieval experiments at 24 °C and at 37 °C, microgroove arrays were placed in an aqueous environment. Although the aqueous solution was removed before the detachment of the arrays from the glass surface, there was liquid remaining underneath the microgrooves. The detachment of the arrays from the deposition substrates may have initiated a liquid flow, which may have subsequently caused hydrodynamic forces. We infer that release of single cells at 37 °C resulted from these hydrodynamic forces. These forces may have disrupted the cells, which were not well interconnected with tissue structures because of less cell–cell and cell–ECM contacts.

To characterize the uniformity of the retrieved modular tissues, the lengths of the retrieved tissue constructs were quantified. A wide distribution in the frequency of lengths of longitudinal tissues was observed, as shown in Figure 6d. This may be due to the hydrodynamic forces in the aqueous environment that occurred during the detachment of microgroove arrays from the deposition surface or due to less cell–cell and cell–ECM interactions. These modular tissues can be convenient models for cardiac tissues,³⁷ myotubes,⁴⁰ myocardium tissues,³² skeletal muscle tissues,³⁴ and capillaries.²⁰ In further studies, using modular tissue engineering methods,⁴¹ it may be possible to assemble these modular tissue units into defined geometries to form more elaborate tissue constructs.

Harvesting tissue constructs from culture platforms with either digestive enzymes or mechanical scraping often causes undesirable effects on cells and their conditioned ECM.^{19,42,43} PNIPAAm-grafted culture substrates were previously used to form tissue structures and detach them from the culture surface by using switchable hydrophilicity/hydrophobicity at two different temperatures.^{19,20} However, a previous coating method on microstructured substrates led to nonconformal PNIPAAm coatings.^{19,20} In this study, PNIPAAm coating with iCVD caused a conformal thin film on PDMS microgrooves which provided a desirable 3D microenvironment for structural organization of the cells to form tissue fibers. In addition, conformally coated rigid PDMS substrates provide an advantage over soft-lithographically fabricated PNIPAAm microstructures²¹ in terms of stability under temperature changes because temperature-dependent

shape changing characteristics of soft-lithographically fabricated PNIPAAm microstructures apply mechanical forces on cell aggregates and may cause deformation on resulting tissue structures.²¹ Furthermore, responsive polymer film exhibited a remarkable swelling change and an increased hydrophilicity at 24 °C compared to 37 °C. This swollen state and increased hydrophilicity of the polymer film caused subsequent retrieval of modular tissue constructs from the grooves. These properties suggest that PNIPAAm deposited PDMS microgrooves may be useful as 3D culture platforms.

CONCLUSION

In summary, conformal coating of PNIPAAm on PDMS microgroove substrates is shown. We demonstrated that these responsive microgrooves can generate tissue fibers and enable their subsequent release in a temperature-dependent manner. Temperature-responsive film on the templates exhibited more swelling and higher hydrophilicity at room temperature compared to physiological temperature. Furthermore, the swollen-state PNIPAAm film with increased hydrophilicity at room temperature initiated the retrieval of modular tissue constructs. This stimuli-responsive template can be potentially integrated with microfluidic devices and may become a versatile tool for various applications that require modular tissue formation and experimentation, such as tissue engineering and drug discovery.

AUTHOR INFORMATION

Corresponding Author

*E-mail: rlanger@mit.edu (R.L.); alik@rics.bwh.harvard.edu (A.K.); MDemirel@engr.psu.edu (M.C.D.).

Author Contributions

[†]These authors contributed equally to this work.

ACKNOWLEDGMENT

We would like to acknowledge financial support from the U.S. Army Research Office through the Institute for Soldier Nanotechnologies at MIT under the project DAAD-19-02-D-002, the Draper Laboratory, the NIH (DE01323, DE016516, HL092836, DE019024, EB007249), the NSF Career Award (DMR0-847287), the Wyss Institute for Biologically Inspired Engineering, and the Office of Naval Research Young Investigator Award.

REFERENCES

- (1) Peppas, N. A.; Langer, R. New challenges in biomaterials. *Science* **1994**, *263* (5154), 1715–1720.
- (2) Hung, P. J.; Lee, P. J.; Sabounchi, P.; Aghdam, N.; Lin, R.; Lee, L. P. A novel high aspect ratio microfluidic design to provide a stable and uniform microenvironment for cell growth in a high throughput mammalian cell culture array. *Lab Chip* **2005**, *5* (1), 44–48.
- (3) Kim, M. S.; Yeon, J. H.; Park, J. K. A microfluidic platform for 3-dimensional cell culture and cell-based assays. *Biomed. Microdevices* **2007**, *9* (1), 25–34.
- (4) Ye, N. N.; Qin, J. H.; Shi, W. W.; Liu, X.; Lin, B. C. Cell-based high content screening using an integrated microfluidic device. *Lab Chip* **2007**, *7* (12), 1696–1704.
- (5) Huh, D.; Matthews, B. D.; Mammoto, A.; Montoya-Zavala, M.; Hsin, H. Y.; Ingber, D. E. Reconstituting organ-level lung functions on a chip. *Science* **2010**, *328* (5986), 1662–1668.

- (6) Lee, J. N.; Park, C.; Whitesides, G. M. Solvent compatibility of poly(dimethylsiloxane)-based microfluidic devices. *Anal. Chem.* **2003**, *75* (23), 6544–6554.
- (7) Wright, D.; Rajalingam, B.; Karp, J. M.; Selvarasah, S.; Ling, Y. B.; Yeh, J.; Langer, R.; Dokmeci, M. R.; Khademhosseini, A. Reusable, reversibly sealable parylene membranes for cell and protein patterning. *J. Biomed. Mater. Res., Part A* **2008**, *85A* (2), 530–538.
- (8) Demirel, G.; Malvadkar, N.; Demirel, M. C. Template-based and template-free preparation of nanostructured parylene via oblique angle polymerization. *Thin Solid Films* **2010**, *518* (15), 4252–4255.
- (9) Ince, G. O.; Demirel, G.; Gleason, K. K.; Demirel, M. C. Highly swellable free-standing hydrogel nanotube forests. *Soft Matter* **2010**, *6* (8), 1635–1639.
- (10) Alf, M. E.; Asatekin, A.; Barr, M. C.; Baxamusa, S. H.; Chelawat, H.; Ozaydin-Ince, G.; Petruczuk, C. D.; Sreenivasan, R.; Tenhaeff, W. E.; Trujillo, N. J.; Vaddiraju, S.; Xu, J. J.; Gleason, K. K. Chemical Vapor Deposition of Conformal, Functional, and Responsive Polymer Films. *Adv. Mater.* **2010**, *22* (18), 1993–2027.
- (11) Ma, D.; Chen, H. W.; Shi, D. Y.; Li, Z. M.; Wang, J. F. Preparation and characterization of thermo-responsive PDMS surfaces grafted with poly(*N*-isopropylacrylamide) by benzophenone-initiated photopolymerization. *J. Colloid Interface Sci.* **2009**, *332* (1), 85–90.
- (12) Lee, E. L.; von Recum, H. A. Cell culture platform with mechanical conditioning and nondamaging cellular detachment. *J. Biomed. Mater. Res., Part A* **2010**, *93A* (2), 411–418.
- (13) Okano, T.; Yamada, N.; Okuhara, M.; Sakai, H.; Sakurai, Y. Mechanism of cell detachment from temperature-modulated, hydrophilic–hydrophobic polymer surfaces. *Biomaterials* **1995**, *16* (4), 297–303.
- (14) Canavan, H. E.; Cheng, X. H.; Graham, D. J.; Ratner, B. D.; Castner, D. G. Surface characterization of the extracellular matrix remaining after cell detachment from a thermoresponsive polymer. *Langmuir* **2005**, *21* (5), 1949–1955.
- (15) Canavan, H. E.; Cheng, X. H.; Graham, D. J.; Ratner, B. D.; Castner, D. G. Cell sheet detachment affects the extracellular matrix: A surface science study comparing thermal liftoff, enzymatic, and mechanical methods. *J. Biomed. Mater. Res., Part A* **2005**, *75A* (1), 1–13.
- (16) Kushida, A.; Yamato, M.; Kikuchi, A.; Okano, T. Two-dimensional manipulation of differentiated Madin–Darby canine kidney (MDCK) cell sheets: The noninvasive harvest from temperature-responsive culture dishes and transfer to other surfaces. *J. Biomed. Mater. Res.* **2001**, *54* (1), 37–46.
- (17) Kushida, A.; Yamato, M.; Konno, C.; Kikuchi, A.; Sakurai, Y.; Okano, T. Decrease in culture temperature releases monolayer endothelial cell sheets together with deposited fibronectin matrix from temperature-responsive culture surfaces. *J. Biomed. Mater. Res.* **1999**, *45* (4), 355–362.
- (18) Ista, L. K.; Perez-Luna, V. H.; Lopez, G. P. Surface-grafted, environmentally sensitive polymers for biofilm release. *Appl. Environ. Microbiol.* **1999**, *65* (4), 1603–1609.
- (19) Isenberg, B. C.; Tsuda, Y.; Williams, C.; Shimizu, T.; Yamato, M.; Okano, T.; Wong, J. Y. A thermoresponsive, microtextured substrate for cell sheet engineering with defined structural organization. *Biomaterials* **2008**, *29* (17), 2565–2572.
- (20) Tsuda, Y.; Yamato, M.; Kikuchi, A.; Watanabe, M.; Chen, G. P.; Takahashi, Y.; Okano, T. Thermoresponsive microtextured culture surfaces facilitate fabrication of capillary networks. *Adv. Mater.* **2007**, *19* (21), 3633–3636.
- (21) Tekin, H.; Anaya, M.; Brigham, M. D.; Nauman, C.; Langer, R.; Khademhosseini, A. Stimuli-responsive microwells for formation and retrieval of cell aggregates. *Lab Chip* **2010**, *10* (18), 2411–2418.
- (22) Alf, M. E.; Godfrin, P. D.; Hatton, T. A.; Gleason, K. K. Sharp hydrophilicity switching and conformality on nanostructured surfaces prepared via initiated chemical vapor deposition (iCVD) of a novel thermally responsive copolymer. *Macromol. Rapid Commun.* **2010**, *31* (24), 2166–2172.
- (23) Sugiura, S.; Imano, W.; Takagi, T.; Sakai, K.; Kanamori, T. Thermoresponsive protein adsorption of poly(*N*-isopropylacrylamide)-modified streptavidin on polydimethylsiloxane microchannel surfaces. *Biosens. Bioelectron.* **2009**, *24* (5), 1135–1140.

- (24) Lydon, M. J.; Minett, T. W.; Tighe, B. J. Cellular interactions with synthetic-polymer surfaces in culture. *Biomaterials* **1985**, *6* (6), 396–402.
- (25) Baier, R. E.; Meyer, A. E.; Natiella, J. R.; Natiella, R. R.; Carter, J. M. Surface-properties determine bioadhesive outcomes - Methods and results. *J. Biomed. Mater. Res.* **1984**, *18* (4), 337–355.
- (26) Schakenraad, J. M.; Busscher, H. J.; Wildevuur, C. R. H.; Arends, J. The influence of substratum surface free-energy on growth and spreading of human-fibroblasts in the presence and absence of serum-proteins. *J. Biomed. Mater. Res.* **1986**, *20* (6), 773–784.
- (27) Klebe, R. J.; Bentley, K. L.; Schoen, R. C. Adhesive substrates for fibronectin. *J. Cell. Physiol.* **1981**, *109* (3), 481–488.
- (28) Pettit, D. K.; Horbett, T. A.; Hoffman, A. S. Influence of the substrate binding characteristics of fibronectin on corneal epithelial-cell outgrowth. *J. Biomed. Mater. Res.* **1992**, *26* (10), 1259–1275.
- (29) Yamato, M.; Konno, C.; Kushida, A.; Hirose, M.; Utsumi, M.; Kikuchi, A.; Okano, T. Release of adsorbed fibronectin from temperature-responsive culture surfaces requires cellular activity. *Biomaterials* **2000**, *21* (10), 981–986.
- (30) Charest, J. L.; Garcia, A. J.; King, W. P. Myoblast alignment and differentiation on cell culture substrates with microscale topography and model chemistries. *Biomaterials* **2007**, *28* (13), 2202–2210.
- (31) Motlagh, D.; Hartman, T. J.; Desai, T. A.; Russell, B. Micro-fabricated grooves recapitulate neonatal myocyte connexin43 and N-cadherin expression and localization. *J. Biomed. Mater. Res., Part A* **2003**, *67A* (1), 148–157.
- (32) Camelliti, P.; Gallagher, J. O.; Kohl, P.; McCulloch, A. D. Micropatterned cell cultures on elastic membranes as an in vitro model of myocardium. *Nat. Protoc.* **2006**, *1* (3), 1379–1391.
- (33) Kim, D. H.; Lipke, E. A.; Kim, P.; Cheong, R.; Thompson, S.; Delannoy, M.; Suh, K. Y.; Tung, L.; Levchenko, A. Nanoscale cues regulate the structure and function of macroscopic cardiac tissue constructs. *Proc. Natl. Acad. Sci. U.S.A.* **2010**, *107* (2), 565–570.
- (34) Bian, W. N.; Liau, B.; Badie, N.; Bursac, N. Mesoscopic hydrogel molding to control the 3D geometry of bioartificial muscle tissues. *Nat. Protoc.* **2009**, *4* (10), 1522–1534.
- (35) Aubin, H.; Nichol, J. W.; Hutson, C. B.; Bae, H.; Sieminski, A. L.; Cropek, D. M.; Akhyari, P.; Khademhosseini, A. Directed 3D cell alignment and elongation in microengineered hydrogels. *Biomaterials* **2010**, *31* (27), 6941–6951.
- (36) Karp, J. M.; Yeo, Y.; Geng, W. L.; Cannizarro, C.; Yan, K.; Kohane, D. S.; Vunjak-Novakovic, G.; Langer, R. S.; Radisic, M. A photolithographic method to create cellular micropatterns. *Biomaterials* **2006**, *27* (27), 4755–4764.
- (37) Khademhosseini, A.; Eng, G.; Yeh, J.; Kucharczyk, P. A.; Langer, R.; Vunjak-Novakovic, G.; Radisic, M. Microfluidic patterning for fabrication of contractile cardiac organoids. *Biomedical Microdevices* **2007**, *9* (2), 149–157.
- (38) Chen, C. S.; Mrksich, M.; Huang, S.; Whitesides, G. M.; Ingber, D. E. Geometric control of cell life and death. *Science* **1997**, *276* (5317), 1425–1428.
- (39) Mooney, D.; Hansen, L.; Vacanti, J.; Langer, R.; Farmer, S.; Ingber, D. Switching from differentiation to growth in hepatocytes - Control by extracellular-matrix. *J. Cell. Physiol.* **1992**, *151* (3), 497–505.
- (40) Huang, N. F.; Patel, S.; Thakar, R. G.; Wu, J.; Hsiao, B. S.; Chu, B.; Lee, R. J.; Li, S. Myotube assembly on nanofibrous and micro-patterned polymers. *Nano Lett.* **2006**, *6* (3), 537–542.
- (41) Nichol, J. W.; Khademhosseini, A. Modular tissue engineering: Engineering biological tissues from the bottom up. *Soft Matter* **2009**, *5* (7), 1312–1319.
- (42) Kikuchi, A.; Okano, T. Nanostructured designs of biomedical materials: Applications of cell sheet engineering to functional regenerative tissues and organs. *J. Controlled Release* **2005**, *101* (1–3), 69–84.
- (43) Von Recum, H. A.; Okano, T.; Kim, S. W.; Bernstein, P. S. Maintenance of retinoid metabolism in human retinal pigment epithelium cell culture. *Exp. Eye Res.* **1999**, *69* (1), 97–107.